

The infrared transmittance model for *in-situ* monitoring of diamond on quartz deposition process

SŁAWOMIR KULESZA

Wydział Matematyki i Informatyki, Uniwersytet Warmińsko-Mazurski,
Żołnierska 14, 10-561 Olsztyn, Poland;
e-mail: kulesza@matman.uwm.edu.pl

A model of the optical transmittance of a diamond/quartz/vacuum system in the infrared range is presented in the paper. The model relies on the attenuation of unpolarized light emitted by the substrate, the intensity of which is subsequently measured by the pyrometer at two close wavelengths. Changes in the film thickness give rise to the phase shift between the waves, which in turn influences the apparent temperature measured by the pyrometer. Periodic variation of the apparent temperature is therefore modeled in order to extract the changes in the film thickness and surface roughness. Another question discussed within the frame of the model is the true temperature estimation in the case of samples with the roughest surfaces.

Keywords: infrared transmittance, pyrometry, surface properties.

1. Introduction

Diamond possesses outstanding properties, among which large index of refraction ($n = 2.45$), extreme hardness, wide band-gap ($E_G = 5.5$ eV), and chemical inertness make it a potential material for many optical applications [1]. However, optical components require strict control of the key parameters of the deposit such as the film thickness, absorption coefficient, and surface roughness. From that point of view, infrared pyrometry appears to be a great tool for *in-situ* monitoring of the quality of deposits.

A number of studies have been performed to provide information on the structural data from measured temperature oscillations [2–6], but they suffer several disadvantages such as: need for calibration run prior to the measurement [2], lack of data on the real emissivity of the sample (single-color pyrometry) [3], assumption that the apparent sample temperature must be equal to the real temperature for large surface roughness [3, 4], assumption that the deposited film is optically flat (no scattering of transmitted light) [3–5], as well as complicated and rather uncertain numerical procedures of fitting experimental data [1, 6].

2. Materials and methods

Diamond samples were grown in a 3 kW ASTeX microwave plasma CVD system (AX 6560). Quartz substrates (1 mm thick) were ultrasonically seeded with 250 nm diamond powder. Gas mixture containing methane diluted with hydrogen was used. The deposition parameters were as follows: CH₄ concentration 1–5 vol%, substrate temperature $T_{\text{sub}} = 500\text{--}920\text{ }^{\circ}\text{C}$, gas pressure $p = 7.33\text{ kPa}$ (55 torr), microwave power $P_{\text{MP}} = 3\text{ kW}$, and deposition time t_{dep} varying from 5 min up to 2 h. Surface morphology was studied using atomic force microscopy (Veeco Multimode 8 system). The sample temperature was measured *in-situ* by a two-color pyrometer (Williamson Pro 92-40) located above the sample at an angle of 40° from the substrate normal.

3. The infrared transmittance model

3.1. Apparent (pyrometric) vs. real temperature

The two-color pyrometer (also called ratio pyrometer or dual-wavelength pyrometer) determines the sample temperature T from the ratio of intensity of light measured at two close wavelengths: $I(\lambda_1)/I(\lambda_2)$, which is governed by the Wien law. The relationship between the measured intensity ratio (referred to as the pyrometric ratio), and the sample temperature T is given by:

$$\frac{I(\lambda_1)}{I(\lambda_2)} = \frac{\varepsilon_1}{\varepsilon_2} \left(\frac{\lambda_2}{\lambda_1} \right)^5 \exp \left[\frac{hc}{kT} \left(\frac{1}{\lambda_2} - \frac{1}{\lambda_1} \right) \right] \quad (1)$$

where $\varepsilon_1, \varepsilon_2$ are the source emittances at $\lambda_1 = 2180.5\text{ nm}$, $\lambda_2 = 2350.5\text{ nm}$, respectively, h is the Planck constant, and k is the Boltzmann constant. Let us define the reference temperature T_0 :

$$T_0 = \frac{hc}{k} \left(\frac{1}{\lambda_1} - \frac{1}{\lambda_2} \right) = 477\text{ K} \quad (2)$$

The two-color pyrometry assumes that the target is a gray-body, *i.e.*, its emissivity at two wavelengths is equal but less than 1 ($\varepsilon_1 = \varepsilon_2 < 1$). Thus, Eq. (1) can be expressed in terms of the reference temperature as:

$$\frac{I(\lambda_1)}{I(\lambda_2)} = \left(\frac{\lambda_2}{\lambda_1} \right)^5 \exp \left(-\frac{T_0}{T} \right) \quad (3)$$

Equation (3) states that the pyrometric ratio depends on the target temperature, but not on its emissivity. Conversely, Eq. (3) allows us to determine the target temperature having the pyrometric ratio being measured. However, in the case of thin films,

the pyrometric ratio is not only a function of the target temperature, but is also affected by the interference occurring within thin layers. As a result, the apparent target temperature periodically changes with increasing film thickness.

In the problem discussed, the light is emitted by a relatively thick quartz substrate heated by the plasma ball. On the other hand, the spectral emissivity of CVD diamond in the range from 2 to 3 μm is below 2% [7], and hence the temperature oscillations measured by the pyrometer must be associated with changes in the optical transmittance of the growing film (assuming constant substrate temperature). The relationship between the measured and real pyrometric ratio is given by:

$$\left. \frac{I(\lambda_1)}{I(\lambda_2)} \right|_{\text{meas}} = \left. \frac{\text{Tr}(\lambda_1)}{\text{Tr}(\lambda_2)} \frac{I(\lambda_1)}{I(\lambda_2)} \right|_{\text{real}} \quad (4)$$

where $\text{Tr}(\lambda)$ is the optical transmittance of the film for a given wavelength.

Substitution of Eq. (3) into Eq. (4) leads us to the formula relating the optical transmittance of the film with the measured (apparent) temperature as well as the real target temperature:

$$\exp\left(-\frac{T_0}{T_{\text{app}}}\right) = \frac{\text{Tr}(\lambda_1)}{\text{Tr}(\lambda_2)} \exp\left(-\frac{T_0}{T_{\text{real}}}\right) \quad (5)$$

According to Eq. (5), the transmittance ratio of the system is given by:

$$\frac{\text{Tr}(\lambda_2)}{\text{Tr}(\lambda_1)} = \exp\left(\frac{T_0}{T_{\text{app}}} - \frac{T_0}{T_{\text{real}}}\right) \quad (6)$$

In that manner, the problem of apparent temperature modulation can be transformed into the problem of attenuation of light transmitted through the multi-layer system.

The influence of the quartz window through which the infrared beam is transmitted from the chamber to the pyrometer needs to be discussed as well. Quartz glass is used since its transmittance within the range 2.0–2.5 μm is better than 0.9, quartz is also highly transparent in the visible range, resistant to various chemicals, and withstands deposition temperatures up to 900 °C. On the other hand, emissivity of quartz substrate approaches 0.9 (the material radiates around 90% of energy compared to the black-body of the same temperature), so it is a good example of the gray body. Hence, around 81% of the infrared energy emitted by the substrate approaches the pyrometer.

Both wavelengths at which the pyrometric ratio is measured are placed as close as possible to each other and set very narrow-banded, so that changing transmittance characteristics in the measurement path are eliminated which makes the temperature

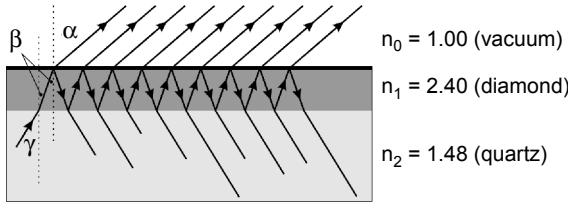


Fig. 1. Schematic cross-section through the diamond on quartz sample, where α is the observation angle, whereas β and γ are appropriate refraction angles within diamond and quartz, respectively.

measurement possible even when there is any interfering factor that reduces radiation from the target including, among others, the window in the deposition chamber.

3.2. A model of optical transmittance

Figure 1 shows a schematic picture of the interfering wavelengths.

Let us assume that the diamond/quartz interface is completely flat (*i.e.*, non-scattering), both materials are homogenous, the diamond is transparent, and its surface is smooth compared to the infrared wavelengths. According to Fresnel equations, the reflection and transmission coefficients for waves parallel (*p*-polarization) and perpendicular (*s*-polarization) to the plane of incidence might be given in the form [8]:

$$r_{10p} = \frac{\tan(\beta - \alpha)}{\tan(\beta + \alpha)}, \quad r_{10s} = -\frac{\sin(\beta - \alpha)}{\sin(\beta + \alpha)} \quad (7)$$

$$r_{12p} = \frac{\tan(\beta - \gamma)}{\tan(\beta + \gamma)}, \quad r_{12s} = -\frac{\sin(\beta - \gamma)}{\sin(\beta + \gamma)} \quad (8)$$

$$t_{10p} = \frac{2 \sin(\alpha) \cos(\beta)}{\sin(\alpha + \beta) \cos(\beta - \alpha)}, \quad t_{10s} = \frac{2 \sin(\alpha) \cos(\beta)}{\sin(\alpha + \beta)} \quad (9)$$

Here, $\alpha = 40^\circ$ is the viewing angle of the pyrometer, $\beta = 15.5^\circ$ is the incidence/multiple reflection angle within diamond film, whereas $\gamma = 26.3^\circ$ is the incidence/multiple reflection angle in quartz. Note that the light emitted by the target is not polarized, and therefore the amplitude (complex) transmission coefficients $\text{tr}(\lambda)$ for multiply reflected beams must be derived separately for each *s*- and *p*-polarized wave in the form:

$$\text{tr}_s = \left(\frac{t_{10s} S_t}{1 - r_{10s} r_{12s} S_r \exp(-i\varphi)} \right)_s \quad (10a)$$

$$\text{tr}_p = \left(\frac{t_{10p} S_t}{1 - r_{10p} r_{12p} S_r \exp(-i\varphi)} \right)_p \quad (10b)$$

where: t_{10} , r_{10} , r_{12} are the appropriate Fresnel coefficients for a given polarization. In the calculations, the following values for index of refraction were used: $n_0 = 1$ (vacuum), $n_1 = 2.4$ (diamond), $n_2 = 1.45$ (quartz). The terms S_t and S_r account for the surface scattering coefficients of light transmitted through and reflected internally from diamond/vacuum interface, respectively. According to the Beckmann–Kirchhoff theory of light scattering, they are functions of the surface roughness σ [9]:

$$S_t = \exp \left\{ -\frac{1}{2} \left[\frac{2\pi(n_1 - n_0)\cos(\alpha)\sigma}{\lambda} \right]^2 \right\} \quad (11a)$$

$$S_r = \exp \left\{ -\frac{1}{2} \left[\frac{4\pi n_1 \cos(\beta)\sigma}{\lambda} \right]^2 \right\} \quad (11b)$$

The phase shift φ in Eq. (10) depends on the films thickness d , and is defined as:

$$\varphi(d) = \frac{4\pi n_1 d \cos(\beta)}{\lambda} \quad (12)$$

The transmittance for the diamond/quartz system at a given wavelength is given by:

$$\text{Tr}(\lambda) = \frac{1}{2} \left(|\text{tr}_s|^2 + |\text{tr}_p|^2 \right) \quad (13)$$

The transmittance ratio takes its final form by dividing the transmittance coefficients calculated for both wavelengths λ_1 and λ_2 :

$$\frac{\text{Tr}(\lambda_2)}{\text{Tr}(\lambda_1)} = \frac{A + B}{C + D} \quad (14)$$

where:

$$A = \left(\frac{(t_{10}S_t)^2}{1 - 2r_{10}r_{12}S_r \cos(\varphi) + (r_{10}r_{12}S_r)^2} \right)_{s, \lambda_2}$$

$$B = \left(\frac{(t_{10}S_t)^2}{1 - 2r_{10}r_{12}S_r \cos(\varphi) + (r_{10}r_{12}S_r)^2} \right)_{p, \lambda_2}$$

$$C = \left(\frac{(t_{10}S_t)^2}{1 - 2r_{10}r_{12}S_r \cos(\varphi) + (r_{10}r_{12}S_r)^2} \right)_{s, \lambda_1}$$

$$D = \left(\frac{(t_{10}S_t)^2}{1 - 2r_{10}r_{12}S_r \cos(\varphi) + (r_{10}r_{12}S_r)^2} \right)_{p, \lambda_1}$$

Equation (14) is the formula for calculating transmittance ratio as a function of the film thickness and the surface roughness.

4. Results and discussion

Figure 2 shows an example of curves of the simulated transmittance ratio. Figure 2a shows interference fringes as the film thickness increases from 0 to 7000 nm, for two values of the surface roughness 0 and 100 nm, respectively. The interference pattern enables identification of turning points. Note that these points are independent of

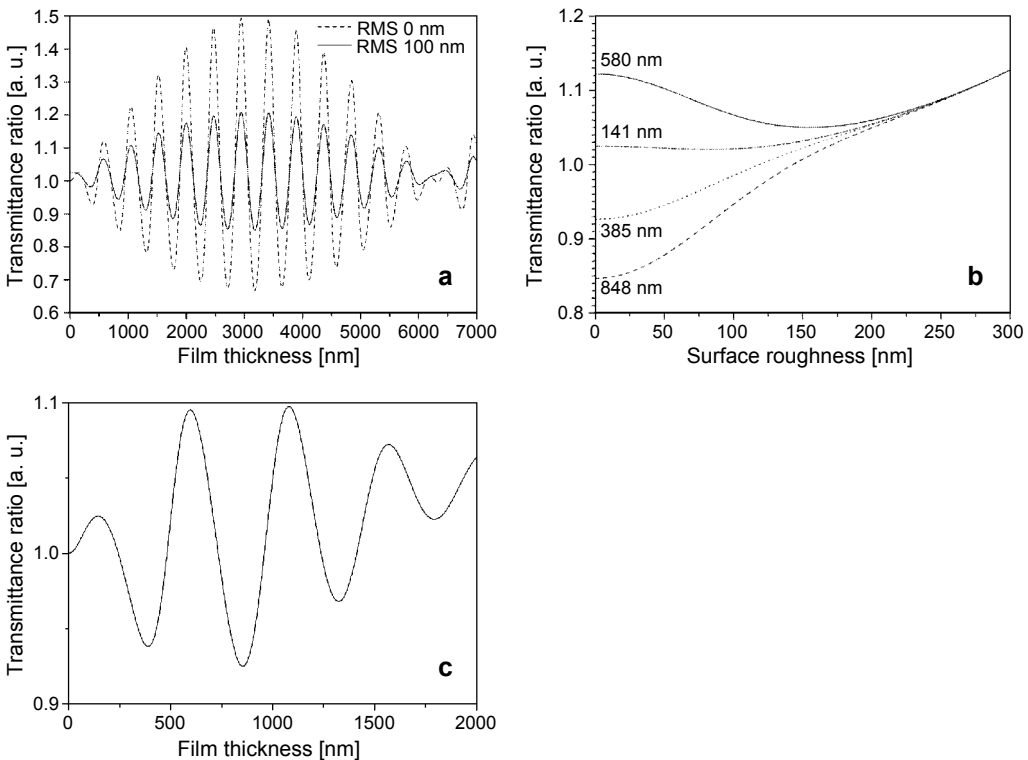


Fig. 2. A series of calculated transmittance ratios for the diamond on quartz structure: the ratio vs. film thickness for the surface roughness fixed at 0 nm (dotted line) and 100 nm (solid line) (a), the transmittance ratio vs. surface roughness for the film thickness fixed at: 141, 385, 580, and 848 nm (at the first four extrema of the left plot) (b), a curve computed as a function of the film thickness for an increasing value of the surface roughness (growth rate is 1 $\mu\text{m}/\text{h}$, surface roughness increases linearly at a rate of 100 nm/h) – note an increasing baseline of the transmittance ratio for larger surface roughness (c).

the surface roughness, even though these curves are rather far from experimental behavior since the roughness increases with increasing deposition time.

In turn, Fig. 2b shows an example of curves computed for surface roughness varying from 0 to 300 nm, having the film thickness fixed at min/max of the interference fringes (*i.e.*, at turning points). Note that each plot increases asymptotically with increasing roughness, *i.e.*, when oscillations are getting damped. Some previous models incorrectly associated a gradual increase of the apparent substrate temperature in the limit of large roughness with increasing real temperature of the growing surface [3, 4]. Moreover, this increase was supposed to contribute to the faster growth rate rather than increasing scattering of light. In fact, our model clearly shows that in the case of rough surfaces the apparent substrate temperature increases leaving the real temperature constant. Since experimental behavior is such that the surface roughness increases with deposition time, Fig. 2c shows a curve simulated for a film grown at a rate of 1 $\mu\text{m}/\text{h}$, and surface roughness increasing at a rate of 100 nm/h, which exhibits asymptotic increase of the transmittance ratio.

Figure 3 shows structural data on the diamond quality. Figure 3a shows a typical Raman spectrum of the diamond under study. Prominent peak at around 1332 cm^{-1} is the main evidence of tetrahedrally bonded carbon atoms (*i.e.*, the diamond structure). According to the formula proposed by VORLICEK *et al.* [10], Raman scattering proves very good quality of diamond films, since the volume fraction of non-diamond phase is less than 2%. In Figure 3b, an example of the AFM image is shown exhibiting the surface roughness of 90 nm.

The transmittance ratio expressed in Eq. (14) was used along with Eq. (6) in order to model the time dependence of the film thickness, growth rate as well as the surface roughness for diamond films grown on quartz substrates. However, due to the numerical complexity of the problem, a semi-empirical approach has been chosen that follows the two consecutive steps: a plot in Fig. 2a was firstly used to assign extrema of measured transmittance ratio to appropriate film thickness, and then, a proper plot in Fig. 2b was used to find out the surface roughness. Figure 4a shows results of such

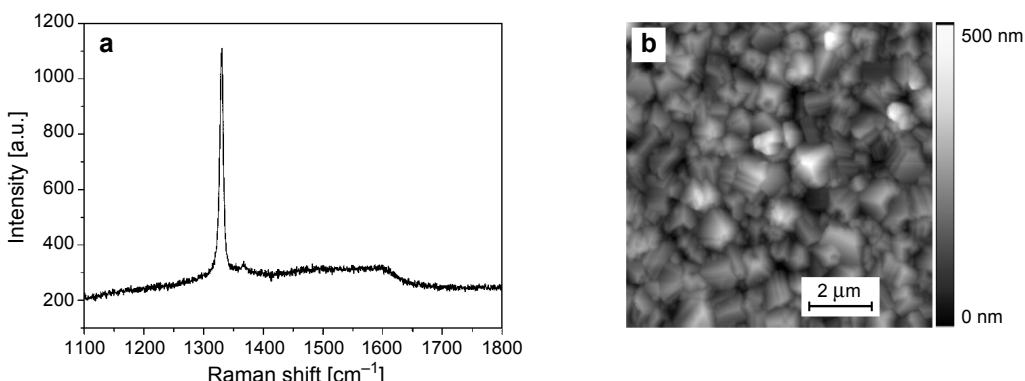


Fig. 3. Raman spectrum of the diamond sample on quartz substrate with the peak at 1332 cm^{-1} (a); AFM image of the sample exhibiting the roughness of 90 nm (b).

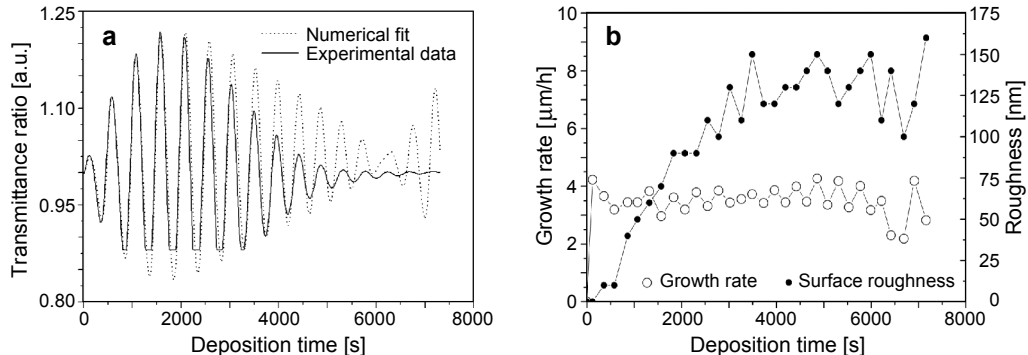


Fig. 4. Graphical verification of the fitting procedure: measured transmittance ratio (solid line), and simulated one (dotted line). A good agreement between both curves is observed for around half of the deposition process, but then a mismatch occurs between roughness data (**a**). Results of the fitting procedure – variations in the growth rate and the surface roughness during the deposition process: the growth rate remains almost constant, whereas the surface roughness initially increases, but then it approaches a constant level (**b**).

a procedure in comparison with experimental data. Even though the cut-off of experimental curve is seen at the level of 0.875 (due to the temperature threshold of the pyrometer), simulated curve reasonably follows the experimental one within at least half of the deposition process, but then the mismatch of oscillation amplitude appears. Such a mismatch is caused by the inaccuracy of roughness estimation, since the positions of the interference fringes of both plots agree very well, and the film thickness does not affect the oscillation amplitude at all (see Fig. 2a).

Figure 4b shows results obtained for the film thickness and the surface roughness using the model discussed. The growth rate of the film remains almost constant within the whole period of deposition process, maintaining $(3.5 \pm 0.8) \mu\text{m/h}$ at 920°C . In contrast to diamond films deposited on carbide-forming substrates (*e.g.*, silicon, titanium) [1, 3], there is no initial period of slowly increasing growth that might eventually indicate a gradual transition between formation of interfacial carbide layer and the actual growth of diamond. Such a result clearly proves that the quartz substrate does not need to be saturated with carbon atoms prior to diamond deposition, which results in faster growth rate (no nucleation induction period), and less contaminated deposit.

The plot of the surface roughness shown in Fig. 4b smoothly increases with time. Within the first 60 min of the deposition, the roughness increases almost linearly, and the rate of this increase is approximately equal to 130 nm/h . This might be associated with the free-growth regime, when the crystal seeds grow up without touching each other (non-continuous film). Then, observed linear dependence saturates, which might be due to the growth regime, when the seeds stick together and compete for the empty space.

Similar analysis has been performed for a variety of diamond samples deposited on quartz substrates. The growth rate was found to increase from 0.35 $\mu\text{m}/\text{h}$ at 500 °C to 3.5 $\mu\text{m}/\text{h}$ at 920 °C, exhibiting a strong correlation with the deposition temperature. Note that the values obtained are generally higher than those measured in a similar configuration for diamond films on silicon [1], presumably because no interfacial carbide layer was formed prior to diamond deposition (no substrate carburization). Moreover, they are at least two times larger than those reported elsewhere for deposition of diamond on quartz substrates [11, 12], which might be due to the pre-treatment procedure (long-lasting mechanical seeding).

In order to verify the model discussed in the paper, a comparison of the roughness data extracted from the pyrometric measurements with those obtained by the AFM measurements has been made. Figure 5a shows the evidence that the surface roughness predicted by the model is only slightly overestimated with respect to what is measured by the AFM. The latter is assumed to exhibit the “true” surface roughness as it exhibits pure topological features of the surface. On that account, the observed overestimation might be due to increasing optical absorption in diamond (assumed to be zero in the model) that enhances light attenuation and adds up to the attenuation caused by the surface scattering. On the other hand, “pure” surface roughness determined from AFM data gives us opportunity of estimating optical constants of diamond (absorption coefficient, index of refraction, extinction coefficient), when analyzed together with total and specular optical transmittance. This problem is to be addressed in further work.

Another comparison is presented in Fig. 5b, where the growth rate obtained using the above model is shown against the growth rate calculated from profilometric measurements of the as-grown samples. Again, the model appears to be consistent with the measured data, although in this case pyrometric results are found slightly

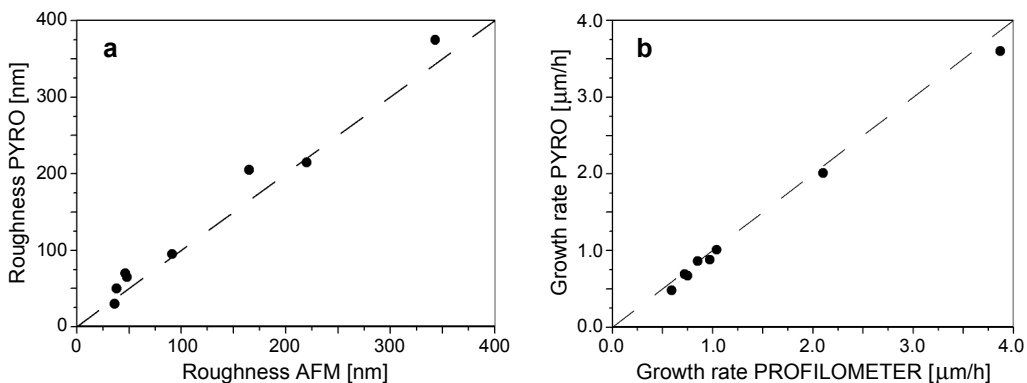


Fig. 5. Comparison of the surface roughness as calculated using the transmittance model and exhibited by the AFM measurements (a); Comparison of the growth rate as calculated using the transmittance model and determined from the profilometric data (b).

underestimated. Several reasons might be responsible for such an effect: uncertain geometry of the problem, variations in the index of refraction of diamond due to non-diamond inclusions, non-flat diamond surface, *etc.*

When it comes to adhesion of diamond films grown on quartz at temperatures 500 °C and higher, linear thermal expansion coefficient for quartz ($0.59 \times 10^{-6} \text{ K}^{-1}$) is lower than for diamond ($1 \times 10^{-6} \text{ K}^{-1}$), which means that the thick substrate expands to lower degree. Hence, thin diamond films with the thickness not exceeding 10 µm suffer from lesser thermal stresses in comparison with, *e.g.*, diamond films deposited on silicon substrates. As a result, diamond layers grown on quartz are flat without cracks and peels (see Fig. 3b).

5. Conclusions

Summarizing, the model of infrared transmittance of the diamond on quartz system is presented in the paper, which explains the oscillations observed in the apparent temperature measured by the two-color pyrometer. The model is used to extract information on the film thickness, surface roughness, and their variations during the deposition process. The obtained growth rate of diamond is found substantially different compared to the case of carbide-forming substrates. Concerning the surface roughness and film thickness (growth rate), the model is consistent with AFM and profilometric data.

References

- [1] MORTET V., KROMKA A., KRAVETS R., ROSA J., VORLICEK V., ZEMEK J., VANECEK M., *Investigation of diamond growth at high pressure by microwave plasma chemical vapour deposition*, Diamond and Related Materials **13**(4–8), 2004, pp. 604–609.
- [2] SPRINGTHORPE A.J., HUMPHREYS T.P., MAJEEDE A., MOORE W.T., *In situ growth rate measurements during molecular beam epitaxy using an optical pyrometer*, Applied Physics Letters **55**(20), 1989, pp. 2138–2140.
- [3] CATLEDGE S.A., COMER W., VOHRA Y.K., *In situ diagnostics of film thickness and surface roughness of diamond films on a Ti–6Al–4V alloy by optical pyrometry*, Applied Physics Letters **73**(2), 1998, pp. 181–183.
- [4] AKKERMAN Z.L., SONG Y., YIN Z., SMITH F.W., GAT R., *In situ determination of the surface roughness of diamond films using optical pyrometry*, Applied Physics Letters **72**(8), 1998, pp. 903–905.
- [5] SNAIL K.A., MARKS CH.M., *In situ diamond growth rate measurement using emission interferometry*, Applied Physics Letters **60**(25), 1992, pp. 3135–3137.
- [6] BENEDIC F., BRUNO P., PIGEAT PH., *Real-time optical monitoring of thin film growth by in situ pyrometry through multiple layers and effective media approximation modeling*, Applied Physics Letters **90**(13), 2007, article 134104.
- [7] CLEMENT R.E., *LWIR spectral properties of CVD diamond at cryogenic temperatures*, Diamond and Related Materials **6**(1), 1997, pp. 169–171.
- [8] BORN M., WOLF E., *Principles of Optics*, 6th Edition, Pergamon Press, Oxford, 1980, pp. 38–53.
- [9] BECKMANN P., SPIZZICHINO A., *The Scattering of Electromagnetic Waves from Rough Surfaces*, Pergamon, New York, 1963, pp. 17–33.

- [10] VORLICEK Y., ROSA J., VANECEK M., NESLADEK M., STALS L.M., *Quantitative study of Raman scattering and defect optical absorption in CVD diamond films*, Diamond and Related Materials **6**(5–7), 1997, pp. 704–707.
- [11] YANG W.B., LÜ F.X., CAO Z.X., *Growth of nanocrystalline diamond protective coatings on quartz glass*, Journal of Applied Physics **91**(12), 2002, pp. 10068–10073.
- [12] NODA M., MARUI A., SUZUKI T., UMENO M., *Deposition of diamond film on silicon and quartz substrates located near DC plasma*, Diamond and Related Materials **14**(11–12), 2005, pp. 1757–1760.

*Received August 12, 2011
in revised form November 24, 2011*